Chemical and Biological Technologies in Agriculture

RESEARCH

Open Access

Effect of polymer water retaining agent on physical properties of silty clay

Wei Huang[1,2], Haoqiang Lai[1,2], Jiaxin Du[1,2], Cuiying Zhou[1,2*], Zhen Liu[1,2*] and Qian Ni[3]

Abstract

Background: Ecological protection of slope surfaces by vegetation is one of the effective methods to reduce soil erosion. However, the surface soil of slope often has the problems of poor structure and low water use efficiency, which is not conducive to plant growth. Super absorbent resin (SAR) as a new type of water retention agent can effectively improve the surface soil of slopes. The study was designed to evaluate the effect and mechanism of SAR on aggregate stability, soil water characteristics and mechanical strength by analyzing the aggregate characteristics, moisture characteristics, microstructure and mechanical properties of SAR-treated soil.

Results: The results show that (1) the volume expansion and shrinkage in the process of water absorption and release of SAR loosened the soil, which improved the microstructure of the soil and increased the aggregate content, while the change of soil pore distribution significantly affected the soil–water characteristics; (2) the fractal dimension and stability of aggregates, the cohesion and internal friction angle of soils all tend to decrease with increasing SAR; and (3) the strong water absorption and retention of SAR increases the water holding capacity of the soil, thus increasing the water availability.

Conclusions: The above research is conducive to further revealing the good role of SAR in improving the surface soil of slope, promoting plant growth and improving the environmental protection effect. It can provide experimental and data support for the application of polymer water retaining agents.

Keywords: Soil improvement, Super absorbent resin, Soil aggregate, Soil–water characteristic curve, Pore distribution

*Correspondence: zhoucy@mail.sysu.edu.cn; liuzh8@mail.sysu.edu.cn

[1] Sun Yat-Sen University, No. 135 XinGangXiLu, Guangzhou 510275, China
Full list of author information is available at the end of the article

Graphical Abstract

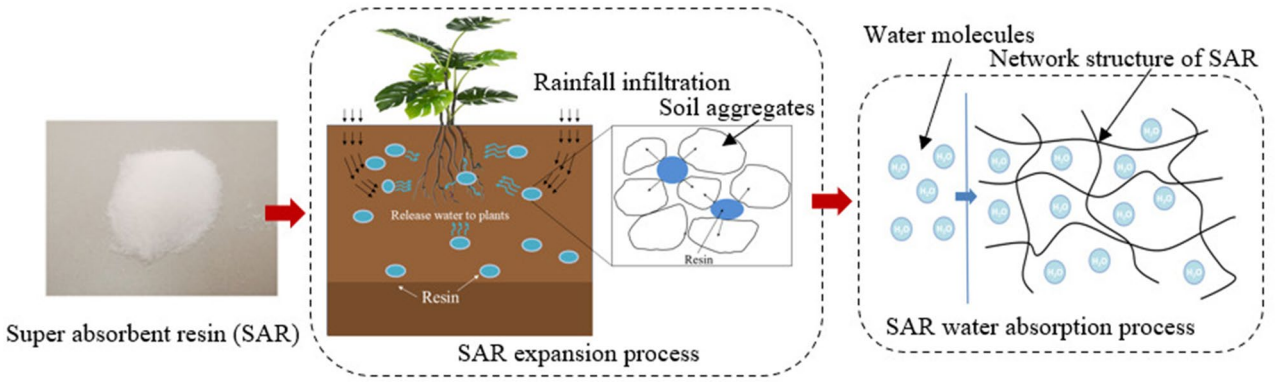

Background

The natural conditions in mountainous areas are complex and the ecological environment is fragile. Large-scale engineering activities will destroy the surface environment, resulting in serious soil erosion [13]. Especially in South China, where rainstorms and climatic droughts occur frequently, these problems are more prominent. Ecological protection technology based on vegetation can effectively protect the surface environment of slopes and reduce soil erosion [12], but the growth of plants needs a good soil environment. Different from intensive cultivation in agricultural engineering, the slope ecological protection project requires deep root depth and high coverage. In general, the technology of soil spraying + native plants is used for rapid greening of the slope to achieve the purpose of soil erosion control and slope ecological protection. Due to the objective conditions such as steep slope, thin soil layer and poor soil, the plant growth environment is generally poor. However, good soil structure and water use efficiency can effectively improve the germination rate and survival rate of plants and promote the growth of plants. Therefore, using an efficient, environmentally friendly and low-cost soil improvement material to improve soil structure and water use efficiency, which is very important to promote plant growth, improve soil and water conservation and ecological protection effect.

In agriculture, conventional soil improvement measures include rotary tillage, fertilization and chemical soil amendments, etc. [19]. Due to the limitations of cost and application conditions, these technologies often have disadvantages such as high cost, long time and poor effect when applied to slope ecological protection engineering. Polymeric water retaining agents as a new type of polymer composites, can absorb and store water through the numerous hydrophilic groups contained in its polymer skeleton, and slowly release water for plant growth when soil lacks water, to improve soil structure and enhance soil water retention performance, it has broad application prospects in the field of slope ecological protection [7]. Hüttermann et al., [4] added superabsorbent material into the soil and found that it could effectively improve the soil water storage capacity, to provide water for plant growth and production. Johnson and Veltkamp, [5] found by scanning electron microscopy that the new polyacrylamide had a cellular structure under expansion conditions, which stored the water in closed vacuoles, to delay the release of water under dry conditions and improve the utilization rate of soil water. Sojka et al. [15] found that polyacrylamide can improve soil structure, and promote the formation of aggregates, thereby increasing soil infiltration and reducing soil surface runoff erosion. Zhang et al. [22] and Kong et al. [6] found through investigation that the water retaining agent can not only retain water and fertilizer but also reduce fertilizer and heavy metal pollution. Yang et al. [21] and Zhao et al. [23] proved that super absorbent material mixed with soil can reduce soil bulk density, and increase soil aggregation, permeability, porosity and water retention capacity. The above research shows that polymer water retaining agents can improve soil water holding capacity, increase the effective water content in the soil, and reduce bulk density, to improve soil structure, promote plant growth, and reduce soil erosion. However, many scholars attribute the increase of soil moisture to water retaining agent, ignoring the enhancement of the water absorption capacity of soil itself caused by structural improvement. Although some scholars have noted that the expansion and contraction of water retaining agents will change the pore connectivity of soil [3], but, due

to the lack of measured data support, the improvement mechanism of water retaining agents on soil structure cannot be accurately described. Moreover, there is little research on the application of water retaining agents in slope ecological protection engineering in South China and its influence on soil aggregates, pore distribution and mechanical properties, which is not conducive to the further promotion and application of polymer water retaining agents in this field.

Based on this, super absorbent resin (SAR) was used as a water retaining agent in this paper to study its improvement effect on aggregate content and stability, pore distribution, water migration and mechanical properties of slope soil. The main material of super absorbent resin (SAR) is sodium polyacrylate, which has the advantages of fast water absorption, large amount and good water retention, and the degradation products are CO_2 and H_2O, which is a soil improvement material with good ecological performance. In this paper, through the analysis of the aggregate characteristics and mechanical properties of modified soil, the influence of SAR on soil aggregate content and stability, and strength were studied. Through the analysis of soil–water characteristics and microstructure, the influence of SAR on pore distribution, microstructure evolution, water availability and soil–water characteristic curve was revealed. The above research is helpful to reveal the good effect of SAR in improving slope soil, promoting plant growth and strengthening slope ecological protection. This study can provide experimentally and data support for the application of polymer water retaining agents.

Table 1 Basic physical properties of silty clay soil

Indexes	Numerical value
Specific gravity *Gs*	2.7
Plastic limit ω_p (%)	22.8
Liquid limit ω_L (%)	36.6
Plasticity index I_p	13.8
Optimum moisture content (%)	17.9
Maximum dry density(g/cm^3)	1.79
Permeability coefficient(cm/s)	6.86×10^{-7}

Source: Geotechnical Test Report of Dejian Reservoir in Qingyuan City, Guangdong Hydropower Planning & Design Institute, 2019.8

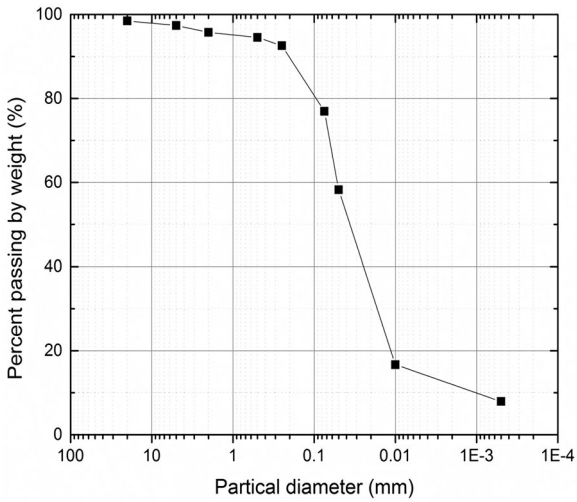

Fig. 1 Gradation curve of silty clay soil

Methods

Test purpose

In this experiment, by analyzing the characteristics of soil aggregates and water, microstructure and mechanical properties, the improvement effect of SAR on soil–water characteristics and mechanical strength of silty clay was studied.

Test material

Test materials include soil and super absorbent resin (SAR).

The test soil was taken from silty clay in Lianshan County, Qingyuan City, Guangdong Province. It is a common red soil in the South Chain, which is weathered by granite. Under natural conditions, the structure is loose and vulnerable to water erosion. The basic physical properties are shown in Table 1. The content of coarse particles in this soil is small, and the content of particles in the range of 0.01–0.2 mm is the largest, accounting for more than 70%. The gradation curve is shown in Fig. 1.

The main component of super absorbent resin (SAR) is sodium polyacrylate. Molecular formula ($C_3H_4O_2$.$C_3H_4O_2$.Na)x (CAS: 9033-79-8), it is a white particle with a diameter of $\leq$ 0.02 mm at room temperature (Fig. 2), moisture content $\leq$ 5%, bulk density 0.8–0.85g/ml. After water absorption and saturation, it was transparent hydrogel. Dry super absorbent resin (SAR) has strong water absorption, which can absorb hundreds of times its weight of water. In addition, the volume of SAR expands when absorbing water, and shrinks when releasing water, which can improve the soil structure. The amount of material added and experimental design are shown in Table 2.

Analysis of soil aggregate characteristics

Soil aggregate content and stability coefficient were determined by the mechanical screening method. The content of non-water stable aggregates was determined by the

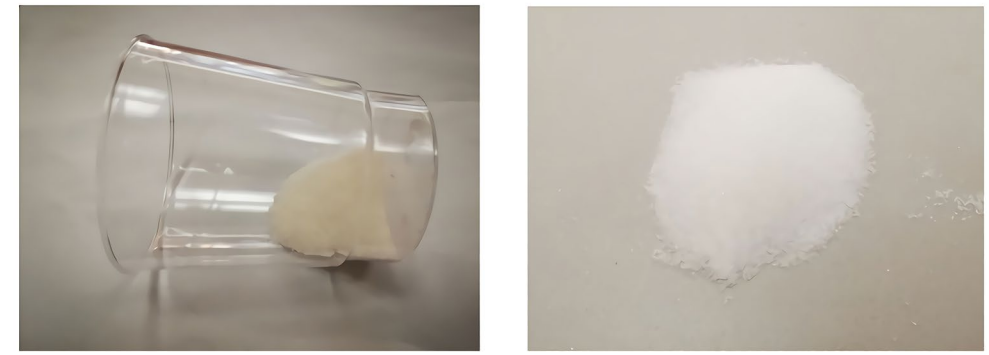

Fig. 2 Pictures of experimental materials super absorbent resin (SAR): (**a**) status in a container and (**b**) status on the plane

Table 2 Amount of material added and experimental design

Test group	SAR addition, mass ratio (%)					Test method	Obtaining parameters
	1	2	3	4	5		
Test contents							
Aggregate characteristic	0	0.025	0.03	0.035	0.04	Dry/Wet sieve method	Water-stable and non-water-stable aggregate content, aggregate fractal dimension and stability coefficient
Water characteristic	0	0.025	0.03	0.035	-	Filter method	Soil–water characteristic curve, water holding capacity and effective water content
Microstructure	0	0.025	0.03	0.035	-	SEM + Data analysis	Microstructure photos and pore distribution
Mechanical characteristics	0	0.025	0.03	0.035	0.04	Direct-shear	Shear strength, cohesion, internal friction angle

Note: the addition amount of SAR (%) = SAR mass/soil mass × 100%

dry sieve method, and the content of water stable aggregates was determined by the wet sieve method [9, 20]. Among them, the pore size of the sieves was: 5, 2, 0.5, 0.25, > 0.25 mm. When wet sieving, the set of sieves was shaken up and down in the water for 30 min at the frequency of 30 times min^{-1}. The soil aggregate parameters were obtained on specimen triplicate and average values were used.

The contents of non-water-stable aggregate [(g/kg)] and water-stable aggregates [M_2 (g/kg)] were calculated according to the following formula:

$$M_1 = \frac{m_1'}{m_1} \times 1000 \quad (1)$$

m_1'—quality of non-water-stable aggregate at all levels, g; m_1—quality of air dried soil samples, g.

$$M_2 = \frac{m_2'}{m_2} \times 1000 \quad (2)$$

m_2'—Quality of water-stable aggregate at all levels, g;m_2—Quality of air dried soil samples, g.

Combined dry and wet sieve methods to simulate the process of rain erosion and calculate the aggregates stability index (*ASI*) [11, 14]:

$$ASI = X_1 + X_2 + X_3 + X_4 + X_5 \quad (3)$$

where X_1, X_2, X_3, X_4, and X_5 represent the probability of soil aggregates stored at > 5, 2, 0.5, 0.25, and > 0.25 mm sieve levels (stability coefficient), respectively.

The calculation formula of fractal dimension (D) of soil aggregates based on particle size weight distribution is as follows [10]:

$$3 - D = lg(W_i/W_0)/lg(d_i/d_{max}) \quad (4)$$

where d_{max} is the average diameter of the maximum grain size particles; d_i is the average particle size of two sieves; W_i is the cumulative mass of soil particle diameter < d_i; W_0 is the mass sum of all soil particles of different grain sizes.

Analysis of soil–water characteristics

Soil matric suction was measured by filter paper method and a soil–water characteristic curve was obtained [8]. Three layers of dried filter paper are placed under the soil sample and made close to the soil sample, of which the upper and lower pieces are protective filter paper and the middle filter paper is test filter paper to keep the filter paper close to the soil sample. The plastic film was wrapped on the outside and placed in the sealing box. After 7 days, the water content of the filter paper and the soil sample was measured. The soil–water parameters were obtained on specimen triplicate and average values were used.

This test uses "Double Circle" No. 203 filter paper, and the matric suction was calculated using the following equations [17]:

$$\begin{cases} logS = 5.493 - 0.0767w_f (w_f \le 47\%) \\ logS = 2.470 - 0.0120w_f (w_f > 47\%) \end{cases} \quad (5)$$

where S is matric suction (kPa) and w_f is water content (%).

Van Genuchten (VG) model (Formula 6) [16] and Gardner (CD) model (Formula 7) [2] were used to fitting the soil–water characteristic curve:

$$\theta = \theta_r + \frac{\theta_s - \theta_r}{[1 + (\alpha S)^n]^m} \quad (6)$$

$$\theta = \theta_r + \frac{\theta_s - \theta_r}{1 + (S/\alpha)^q} \quad (7)$$

where θ—moisture content by volume(%); θ_r—residual volumetric water content(%); θ_s—saturated volumetric water content(%); α, m, n, q—model parameter, and where $m = 1 - 1/n$.

Analysis of soil microstructure

Assuming that the pores in the soil are regular circular pipes, the relationship between suction S (kPa) and capillary diameter D (mm) can be expressed as

$$S = \frac{4\sigma}{D} \quad (8)$$

where σ is the surface tension coefficient of water, which is 0.072 N/m at 25 °C.

The interaction between super absorbent resin (SAR) and soil was observed by scanning electron microscope (SEM). Use of JSM-6330F cold field scanning electron microscope produced by JEOL. The operating conditions of SEM were as followings: an accelerating voltage of 20 kV and a specimen current of 200uA. Representative SEM images were selected to show the morphological characteristics of the improved soil.

Soil strength analysis

The shear strength of improved soil was tested by direct shear apparatus produced by Nanjing Soil Instrument. Mix the SAR into the soil evenly according to Table 2 and fill in the plastic box with the length, width and height of 54 × 36 × 10 cm. To simulate the soil state under natural conditions, soil samples were maintained for 30 days under outdoor conditions. According to the Standard for national criterion for geotechnical tests in China which was set based on ASTM standards (GB/T 50123-, 1999), take soil from a plastic box and carry out the test according to the requirement of undisturbed soil. The sample size is 61.8 mm in diameter and 20 mm in height, and the moisture content of the sample is 17%. The tests were carried out at a strain rate of 0.8 mm/min under the normal pressures of 100, 200, 300 and 400 kPa to define

Table 3 Particle size distribution of soil aggregates

Test groups	SAR(%)	Sieving method	≥ 5 mm	2–5 mm	0.5–2 mm	0.25–0.5 mm	< 0.25 mm	Aggregates stability index (ASI)	Fractal dimension (*D*)
1	0	Dry	27.16 ± 0.1	10.19 ± 0.0	23.53 ± 0.0	7.15 ± 0.0	31.97 ± 0.1	0.180	2.636
		Wet	13.4 ± 0.1	12.11 ± 0.0	19.77 ± 0.0	9.82 ± 0.0	44.9 ± 0.1		2.718
2	0.025	Dry	31.41 ± 0.2	16.33 ± 0.0	24.89 ± 0.1	7.79 ± 0.0	19.58 ± 0.2	0.173	2.506
		Wet	15.24 ± 0.1	16.48 ± 0.0	31.68 ± 0.0	13.15 ± 0.0	23.45 ± 0.1		2.539
3	0.03	Dry	32.84 ± 0.2	18.07 ± 0.0	25.66 ± 0.0	8.37 ± 0.1	15.06 ± 0.1	0.170	2.437
		Wet	16.99 ± 0.1	17.59 ± 0.0	32.25 ± 0.0	12.73 ± 0.0	20.44 ± 0.2		2.503
4	0.035	Dry	32.37 ± 0.1	21.82 ± 0.0	25.78 ± 0.0	8.65 ± 0.0	11.38 ± 0.1	0.167	2.361
		Wet	17.26 ± 0.2	17.64 ± 0.0	32.69 ± 0.1	12.12 ± 0.0	20.29 ± 0.2		2.500
5	0.04	Dry	34.18 ± 0.1	21.43 ± 0.0	25.94 ± 0.0	8.99 ± 0.1	9.46 ± 0.2	0.162	2.316
		Wet	17.31 ± 0.0	17.72 ± 0.0	33.54 ± 0.0	12.06 ± 0.0	19.37 ± 0.1		2.487

the shear strength parameters (c and ψ). In addition, the shear strength parameters were obtained on specimen triplicate and average values were used.

Results

Characteristics of soil aggregates

The effect of super absorbent resin (SAR) on soil aggregate content is shown in Table 3. In each test group, the contents of non-water-stable aggregates with pore sizes of 5, 2, 0.5, 0.25 and > 0.25 mm were 68.03%, 80.42%, 84.94%, 88.62% and 90.54%, respectively. After adding SAR, the content of aggregates at all levels was greater than that of natural soil and was positively correlated with the content of SAR. With the increase of SAR content, the content of aggregates with particle size ≥ 5 mm increased first, then decreased and then increased, but were higher than the natural soil, indicating that SAR was beneficial to increasing the content of aggregates with particle size ≥ 5 mm in silty soil. Aggregate content of 2–5 mm particle size increased first and then decreased with the increase of SAR, and the 4 group was the highest (21.82%). The content of aggregates with a particle size of 0.5–2 mm and 0.25–0.5 mm were 23.53–25.94% and 7.15–8.99%, respectively, and the aggregate contents of the soil samples treated with SAR were greater than those of the control group and increased with the amount of SAR incorporated. It may be because the SAR forms hydrogel after absorbing water, the surface area increases, and adsorbs more small soil particles, thus forming large aggregates.

In each test group, the contents of water-stable aggregates with pore sizes of 5, 2, 0.5, 0.25 and > 0.25 mm were 55.1%, 76.55%, 79.56%, 79.71% and 80.63%, respectively. The content of aggregates after adding SAR was higher than that of the natural soil, and the content of aggregates with particle sizes ≥ 5 mm, 2–5 mm and 1–2 mm were positively correlated with the content of SAR. The aggregate content of 0.25–0.5 mm and 0.5–1 mm increased first and then decreased with the increase of SAR.

By comparing the content of water-stable and non-water-stable aggregates with particle size ≥ 0.25 mm in each test sample, it can be seen that the content of aggregates after adding SAR was higher than that in the natural soil. Although part of the particle size did not change linearly with the content of SAR, the improvement of soil structure can still be seen.

Soil–water characteristic curve

The drying curves of samples added with super absorbent resin (SAR) were higher than those of the natural soil (Fig. 3), and the difference was more significant with the increase of SAR content.

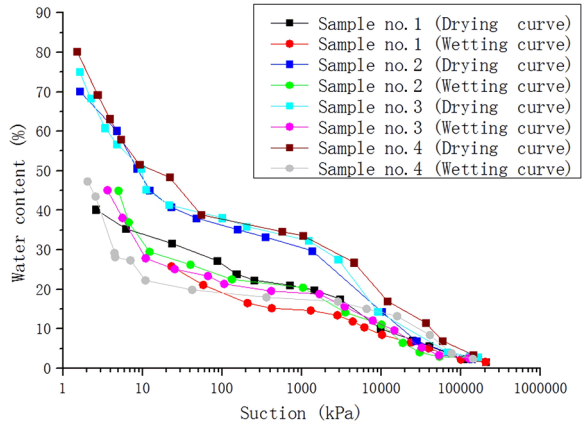

Fig. 3 Soil–water characteristic curve(s)

Compared with the natural soil, the final water absorption of samples no. 2–4 increased by 74.3%, 86.7% and 99.5%, respectively. The wetting curve also has a similar trend: Compared with natural soil, the final water absorption of samples no. 2–4 increased by 74.1%, 74.6% and 83.2%, respectively. This is because, as a water storage material, SAR has the characteristics of high water absorption. It can continuously provide water for the soil under dry conditions. Moreover, SAR not only adsorbs a large amount of water but also changes the soil structure and enables it to accommodate more water by volume change during water absorption and release.

In the low suction section, the material has a significant impact on the soil–water characteristic curve, and in the high suction section, the soil–water characteristic curve of each sample has little difference. Therefore, selecting the middle suction section to analyze the effect of material on soil water retention is the most intuitive. When the suction of the drying curve is 1000 kPa, the water content of treated soil increases by 42.15–56.95% compared with natural soil; And when the suction of the wetting curve is 1000 kPa, the water content of treated soil decreases by 19.61–48.37% compared with natural soil.

Soil structure characteristics

The hysteresis phenomenon of the soil–water characteristic curve during the drying and wetting process reflects the uneven degree of soil pore structure. In general, the more obvious the hysteresis phenomenon is, the higher the unevenness of soil pore size is; On the contrary, it indicates that the soil is rich in fine particles and has uniform pores. It can be seen from Fig. 4 that the hysteresis loop of the soil–water characteristic curve mixed with SAR is significantly larger than that of the natural

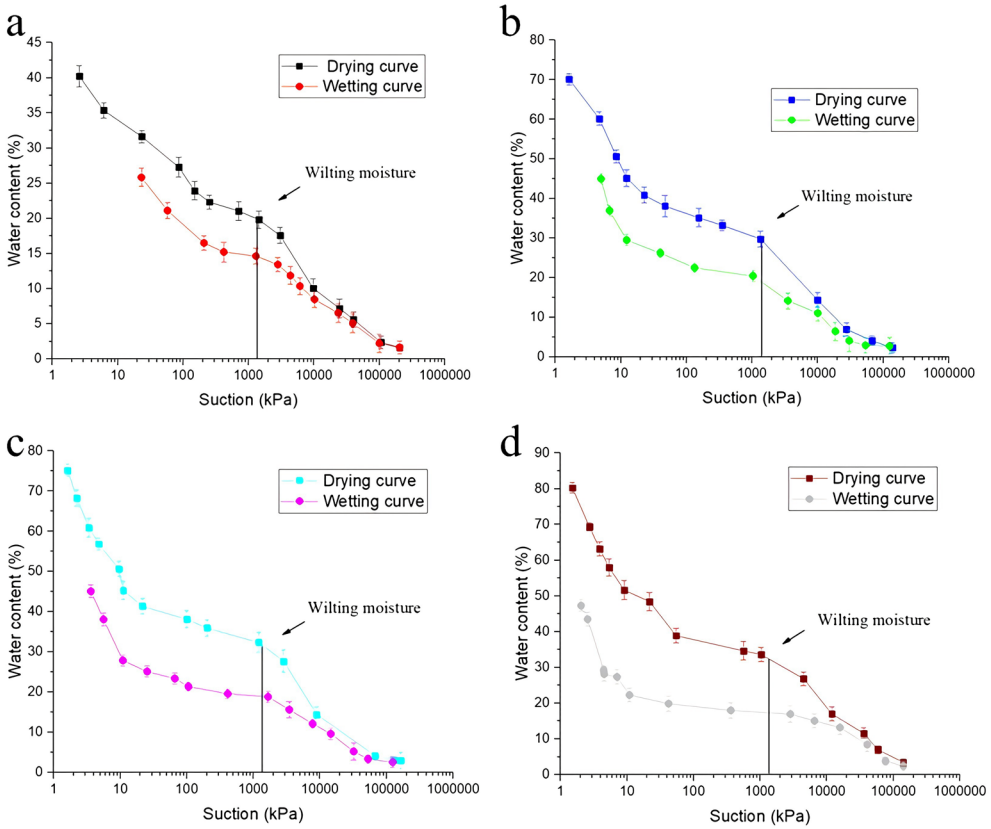

Fig. 4 Soil–water characteristic curve(s): (**a**) sample no. 1, (**b**) sample no. 2, (**c**) sample no. 3, (**d**) sample no. 4

Table 4 Soil pore classification and its changes

Pore type	Aeration pore	Capillary pore	Inactive pore	Total porosity (%)
Equivalent pore size (mm)	> 0.06	0.06–0.002	< 0.002	
Suction pressure(kPa)	4.8	4.8–144	144	
Porosity/proportion (%)				
1	3.16 ± 0.26/7.86 ± 0.65%	22.45 ± 0.3/55.81 ± 0.75%	14.62 ± 0.19/36.33 ± 0.47%	40.23 ± 0.25
2	12.03 ± 0.3/17.16 ± 0.43%	19.42 ± 0.14/27.70 ± 0.2%	38.66 ± 0.27/55.14 ± 0.39%	70.11 ± 0.24
3	16.18 ± 0.24/21.55 ± 0.32%	16.45 ± 0.22/21.90 ± 0.29%	42.48 ± 0.21/56.55 ± 0.28%	75.11 ± 0.22
4	17.35 ± 0.34/21.62 ± 0.42%	18.19 ± 0.27/22.67 ± 0.34%	44.7 ± 0.34/55.71 ± 0.42%	80.24 ± 0.32

Proportion (%) = porosity/total porosity × 100

soil, and is positively correlated with the dosage of SAR. This is because the swelling and shrinking effect of SAR improves the soil structure, forms many large pores in the soil, and increases the heterogeneity of soil pores.

Based on the soil–water characteristic curve, the distribution of soil pores can be obtained by Eq. 8 (Table 4). It can be seen that with the increase of the dosage of SAR, the number of aeration pores and inactive pores increases, while the variation trend of capillary pores is not obvious. Comparing the proportion of soil pores, it can be seen that compared with natural soil (Aeration pores, Capillary pores and Inactive pores are 7.86%, 55.81%, 36.33% in turn), the addition of SAR will increase the proportion of aeration pores (17.16–21.62%) and inactive pores (55.14–56.55%), and reduce the proportion of capillary pores (21.9–27.70%). This is because the volume expansion of SAR in the soil will squeeze the surrounding soil [3], forming many visible pores, and

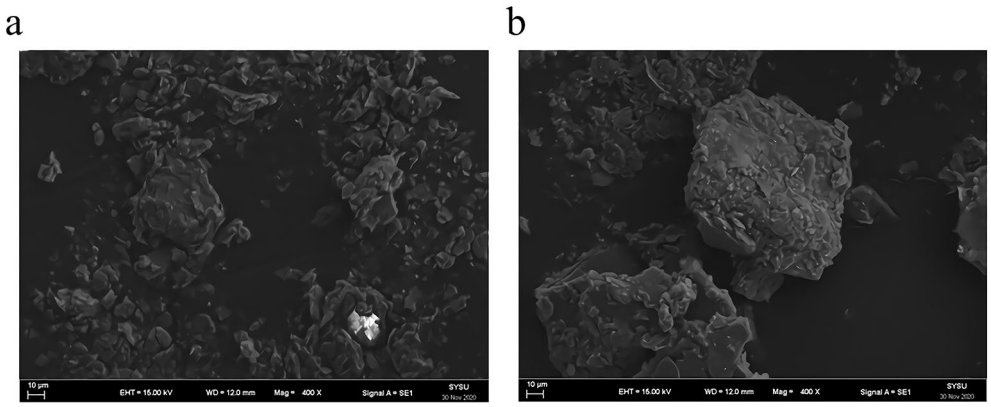

Fig. 5 Scanning electron microscope pictures of soil: (**a**) natural soil(400 times) and (**b**) Sample no. 3 (400 times)

damaging the original soil structure, thus forming a large number of aeration pores. This process is mainly macro-scale pore volume changes, mainly aeration pore, capillary pores and inactive pores also have a certain impact.

The scanning electron microscope (SEM) pictures of the soil before and after improvement are shown in Fig. 5, which shows the improvement effect of SAR on soil structure and morphology.

It can be seen from the picture that the addition of SAR into the soil will lead to a significant decrease in small particles with particle size less than 20 um, and an increase in particles with particle size more than 40

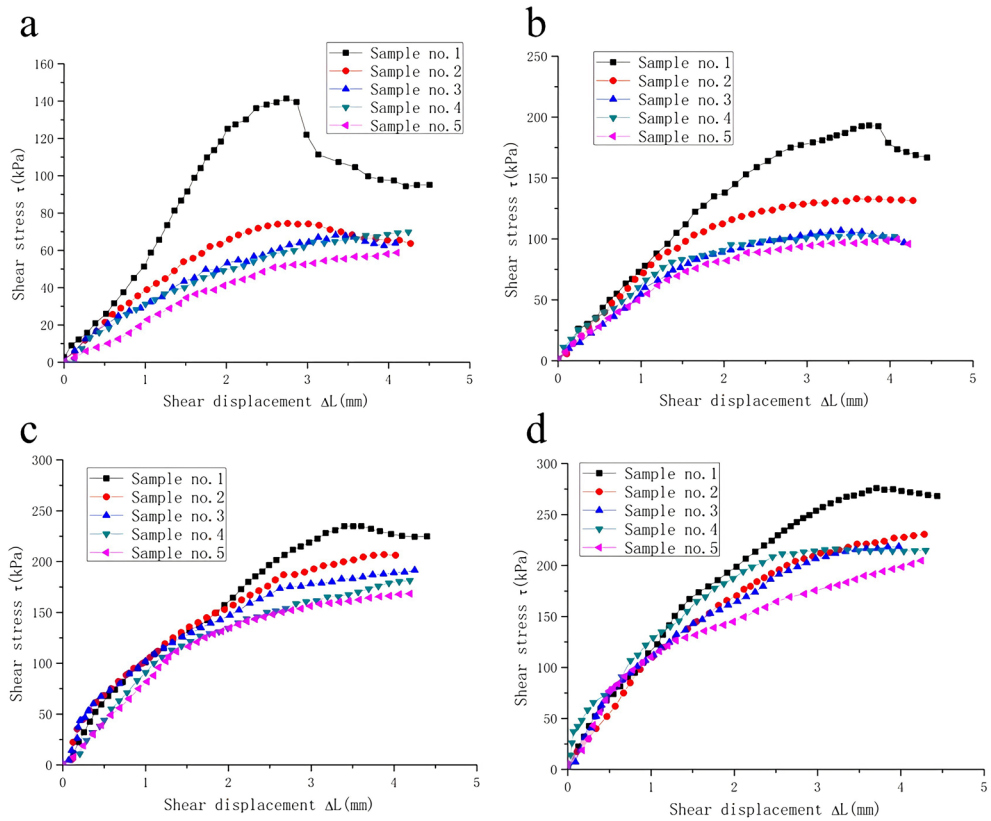

Fig. 6 Stress–strain curves of samples: (**a**) 100 kPa normal stress, (**b**) 200 kPa normal stress, (**c**) 300 kPa normal stress, (**d**) 100 kPa normal stress

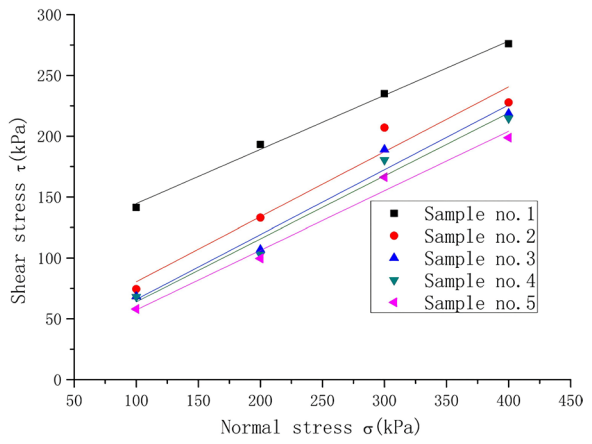

Fig. 7 Shear strength curves of the test groups

Table 5 Cohesion and internal friction angle

Test groups	Cohesion (kPa)	Internal friction angle (°)
1	100.05 ± 2.13	24.01 ± 0.05
2	27.13 ± 1.84	28.08 ± 0.11
3	12.68 ± 1.21	28.03 ± 0.08
4	12.19 ± 0.99	27.35 ± 0.09
5	8.495 ± 0.98	26.04 ± 0.06

um. It shows that SAR can effectively reduce the number of loose fine particles, and increase the number of soil aggregates and the average particle size of aggregates.

Soil mechanical characteristics

The shear strength of soil reflects the difficulty of soil being damaged by shear deformation under external force. Figure 6 shows shear strength and shear displacement curves.

As can be seen in Figs. 6, 7 and Table 5, SAR will lead to varying degrees of decrease in peak shear strength and cohesion of soil, although the SAR can improve the internal friction angle, it also shows a downward trend with the increase of dosage. Comparing the peak strength of each sample under different normal stress, it can be found that the effect of SAR on the peak strength of soil tends to decrease with the increase of axial load. When the normal stress was 100 kPa, 200 kPa, 300 kPa and 400 kPa in turn, compared with natural soil, the peak strength of each sample added with the SAR decreased by 47.36–58.96%, 31.16–48.44%, 11.91–29.24% and 17.51–28.00%, respectively. This is because the mechanical properties of soil are mainly determined by the skeleton of particles. The water absorption expansion of SAR will destroy the skeleton structure, but higher normal stress can alleviate this change.

Discussion

Effects of SAR on soil aggregate characteristics and stability coefficient

Soil aggregate is the basic unit of soil structure, and its stability affects soil strength and anti-erosion ability, which is regarded as one of the important evaluation indexes of soil anti-erosion ability [18]. It also has significant effects on water, fertilizer and other conditions required for plant growth and the environment. Compared with the results of dry-sieving, the content of aggregates in each group with particle size ≥ 0.25 mm in the wet-sieving decreased (Table 3), which was due to the action of the swelling force of the SAR, the aggregates collapsed and formed smaller aggregates. Taking the sample no. 5 as an example, it was found that the proportions of particle size ≥ 5 mm and 2–5 mm decreased by 16.87% and 3.71%, respectively, under the wet-sieving test, and the proportions of particle size 1–2 mm, 0.25–0.5 mm and < 0.25 mm increased by 7.86%, 3.07% and 9.91%, respectively, and the proportions of soil aggregates with a particle size of 0.5–1 mm remained basically unchanged. Other samples also have similar rules. This indicated that under the wet-sieving test, although the aggregates at each particle size were disintegrated, the number of small aggregates is complemented by the disintegration of large particles. Therefore, particle size ≥ 5 mm and 2–5 mm soil aggregate content decreased significantly. The fractal dimension of aggregates under the dry-sieving test was 2.316–2.636, the fractal dimension of aggregates under the wet-sieving test was 2.487–2.718 (Table 3), and the stability coefficient of aggregates was 0.162–0.18. Whether dry or wet sieve, with the increase of resin content, the fractal dimension and stability coefficient of aggregates decreased. This shows that the addition of SAR will destroy the structure of aggregates and reduce the stability of aggregates so that it is more likely to break into smaller aggregates.

The above analysis shows that the addition of SAR in soil has positive and negative effects on soil aggregates. Positive effects: SAR has a significant promoting effect on the formation of soil aggregates. With the increase of SAR content, the number of aggregates in the soil increases significantly. These aggregates have a good effect on improving soil structure, improving soil erosion resistance, preventing surface crust and inhibiting soil evaporation. Negative effects: The increase in SAR will significantly reduce the stability of aggregates, making them more vulnerable to destruction.

Effects of SAR on plant effective water

The soil–water characteristic curve expresses the relationship between matric suction and soil water content, which can reflect the water holding capacity of soils, and can also understand the characteristic index of soil. In general, the suction range of SAR for water is 10 kPa–50 kPa, and the maximum suction range is 400 kPa–1200 kPa. However, the drying and wetting curves begin to change near the suction of 1000 kPa–4000 kPa (Fig. 3). This reflects the change in soil structure caused by SAR, which leads to the change in the soil–water characteristic curve.

At present, the water content corresponding to the suction of 15 bar (1500 kPa) is regarded as the wilting coefficient. In general, when the soil water content is reduced to the wilting coefficient, the plant will not survive. Comparing the soil–water characteristic curves of different SAR additions in Fig. 4 (Drying curve), compared with the natural soil, the water content of plant wilting increased by 50.75–55.78%. However, it can be seen from Fig. 3 that the soil–water characteristic curve with the addition of SAR was significantly higher than that of the natural soil, indicating that the soil water content increased under the same suction condition, and the increase of wilting water content was lower than that of soil water content; therefore, the available water increased by 133.7–158.84%. The wetting curve also has the same trend. When the suction was 1500 kPa, compared with the natural soil, SAR increased the water content of plant wilt by 14.09–33.56%, but the available water content increased by 125.88–178.24%.

Effect of SAR on soil–water characteristic curve fitting

Van Genuchten (VG) model and Gardner (GD) model were used to fitting the soil–water characteristic curve, and the results are shown in Table 6. The goodness of fit (R^2) of Van Genuchten model is not less than 0.944, and the goodness of fit (R^2) of Gardner model is not less than 0.821. Therefore, these two models can describe the soil–water characteristic curve of SAR improved soil, and the VG model fitting effect is better.

Table 6 Fitting results

Test groups	Model	*a*	*n* or *q*	R^2
1	Van genuchten	0.036	1.223	0.953
	Gardner	449.2	0.3819	0.9748
2	Van genuchten	7.185	1.181	0.949
	Gardner	191.7	0.7176	0.8578
3	Van genuchten	4.173	1.175	0.944
	Gardner	204.7	0.5875	0.8682
4	Van genuchten	3.071	1.171	0.956
	Gardner	195.5	0.7126	0.821

Parameter '*a*' of VG model is negatively correlated with intake value [1, 16], the increase of '*a*' indicates that the difficulty of soil water loss is reduced and the water retention of soil is weakened. As can be seen from Table 6, the parameter '*a*' will be significantly improved by adding SAR, but with the increase of SAR content, the parameter '*a*' shows a decreasing trend.

As a kind of high-absorbent material, although the expansion of SAR leads to the increase of soil porosity and the decrease of the air intake value. But, SAR is hydrogel in a saturated state, with the increase of SAR content, a large number of hydrogel blocks pores forms negative pressure, prevents water outflow, and improves the intake value [3].

Figure 8 shows the relationship between suction and soil water content under different additions. In the field conditions, it is difficult to obtain the suction, and the water content is easy to obtain. Therefore, the fitting equation based on the measured data can quickly determine the suction of soil under different water content.

Effect of SAR on soil structure

SAR has the characteristics of hydrophilic expansion and is insoluble in water. It has a spatial three-dimensional network structure, hydrophilic groups (such as $-OH$, $-COOH$, $-CONH_2$, etc.) are distributed on its main or side chain, which can combine with water in nature. In the initial stage of SAR absorption, capillary adsorption played a dominant role, and the absorption rate of SAR was slow. With the increase of water, the chemical structure of SAR began to play a dominant role. The hydrophilic groups on the polymer chain were ionized and hydrogen bonds were generated between water molecules. Water molecules were adsorbed in the three-dimensional network of SAR under the action of hydrogen bonds, and the water absorption and water absorption rate were significantly increased. The water absorbed by SAR exists in three forms: strong binding water, weak binding water and free water. Among them, the SAR has a weak ability to absorb free water (about 85–90%), which is effective water for the plant.

As shown in Fig. 9, the volume of the SAR in the soil expands after water absorption, and it changes from solid particles to hydrogel. In this process, the surrounding soil particles are squeezed by the SAR, and the skeleton structure between the particles will change. Under the effect of a resin expansion force, some of the original inactive pores will be reconnected into capillary pores or aeration pores. At the same time, the specific surface area of SAR increased, and the contact area with soil particles

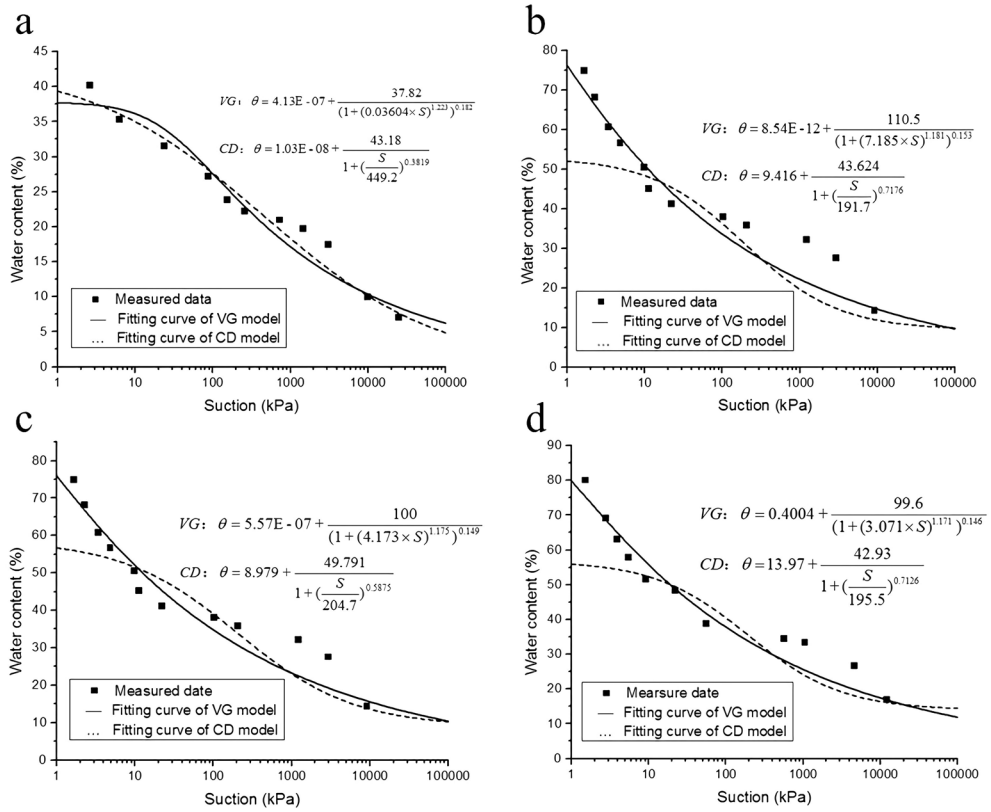

Fig. 8 Fitting results of VG model and CD model: (**a**) drying curve of sample no. 1, (**b**) drying curve of sample no. 2, (**c**) drying curve of sample no. 3, (**d**) drying curve of sample no. 4

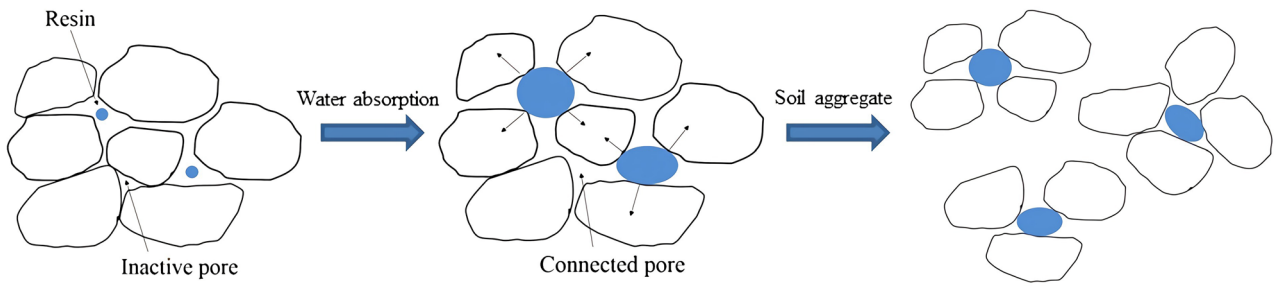

Fig. 9 Expansion and adsorption mechanism of resin in soil

increased. Under the action of capillary action and matrix suction, loose small particles in the soil would adsorb on the SAR surface to form soil aggregates, increasing the number of aggregates in the soil.

Effect of SAR on soil strength

From Fig. 7 and Table 5, it can be seen that SAR can lead to a significant decrease in soil cohesion and an increase in internal friction angle, but with the increase in SAR content, the internal friction angle also showed a downward trend. The shear strength of soil is mainly composed of cohesion and friction between soil particles. The cohesion is related to van der Waals, coulomb, cementation force and osmotic pressure caused by concentration difference, while the friction between soil particles is related to the relative position between particles.

The volume expansion of SAR will lead to bulk expansion, resulting in lower soil density and cohesion; But the expansion force of SAR will squeeze some soil particles so that the original occlusion state increases and

the friction force increases. However, with the increase in SAR content, the damage caused by expansion is greater than that caused by reinforcement. More and more soil particle skeletons are destroyed by extrusion, and the friction force is reduced. Overall, the addition of SAR will lead to a certain degree of ' degradation ' of soil strength, so, the other factors need to be integrated to obtain the optimal dosage of SAR within an acceptable strength range.

Conclusions

This study aimed to investigate the effects of super absorbent resin (SAR) on soil aggregate content and stability, microscopic pore distribution, water migration and mechanical properties. The following are some significant findings:

(1) Super absorbent resin (SAR) can significantly increase the content of water-stable and non-water-stable aggregates, but the fractal dimension and stability coefficient of aggregates decreases with the increase of super absorbent resin (SAR) content.

(2) Adding super absorbent resin (SAR) can improve the drying and wetting curve of soil, and increase the water retention capacity of the soil. Through the fitting analysis of the soil–water characteristic curve, it is found that adding super absorbent resin (SAR) can improve the intake value of soil, but the intake value tends to decrease with the increase of dosage, and the water holding capacity of soil is improved; Van Genuchten (VG) model is more suitable for simulating soil–water characteristic curve of super absorbent resin (SAR) modified soil.

(3) Super absorbent resin (SAR) can significantly improve the total porosity of soil and reduce the uniformity of soil pores, mainly improving the aeration pores with an equivalent pore size greater than 0.06 mm and the inactive pores with a pore size less than 0.002 mm. The volume fluctuation can reduce the uniformity of soil pores.

(4) Super absorbent resin (SAR) can reduce the shear strength of soil, and the cohesion and internal friction angle decrease with the increase of super absorbent resin (SAR) content.

(5) As a soil improver, super absorbent resin (SAR) can reduce soil strength and aggregate stability, but it can promote plant growth by increasing soil aggregate content, improving soil structure and improving water availability, and improving the soil and water conservation and ecological protection effect of the slope.

Acknowledgements
Not applicable.

Author contributions
WH carried out part of the experiments and wrote the manuscript. HQL, JXD, and QN carried out part of the experiments and wrote and revised the manuscript. ZL, and CYZ acquired funding and supervised and revised the work. All authors read and approved the final manuscript.

Funding
This research is supported by Major Programs Special Funds of Applied Science and Technology Research and Development of Guangdong Province (No. 2015B090925016); The National Key Research and Development Project of China (No. 2017YFC1501201); The National Key Research and Development Project of China (No. 2017YFC0804605).

Availability of data and materials
All data generated or analyzed during this study are included in this published article.

Declarations

Ethics approval and consent to participate
Not applicable.

Consent for publication
Not applicable.

Competing interests
The authors declare that they have no competing interests.

Author details
[1]Sun Yat-Sen University, No. 135 XinGangXiLu, Guangzhou 510275, China. [2]Guangdong Engineering Research Centre for Major Infrastructure Safety, Sun Yat-Sen University, Guangzhou 510275, China. [3]School of Civil Engineering, Chongqing Jiaotong University, Chongqing 400074, China.

Received: 15 April 2022 Accepted: 7 June 2022
Published online: 14 July 2022

References

1. Cao J, Jung J, Song X, Bate B. On the soil water characteristic curves of poorly graded granular materials in aqueous polymer solutions. Acta Geotech. 2018. https://doi.org/10.1007/s11440-017-0568-7.
2. Gardner WR. Some steady-state solutions of the unsaturated moisture flow equation with application to evaporation from a water table. Soil Sci. 1958. https://doi.org/10.1097/00010694-195804000-00006.
3. Huang W, Liu Z, Zhou C, Yang X. Enhancement of soil ecological self-repair using a polymer composite material. CATENA. 2020. https://doi.org/10.1016/j.catena.2019.104443.
4. Hüttermann A, Zommorodi M, Reise K. Addition of hydrogels to soil for prolonging the survival of Pinus halepensis seedlings subjected to drought. Soil Tillage Res. 1999. https://doi.org/10.1016/S0167-1987(99)00023-9.
5. Johnson MS, Veltkamp CJ. Structure and functioning of water-storing agricultural polyacrylamides. J Sci Food Agric. 1985;36:789–93. https://doi.org/10.1002/jsfa.2740360905.
6. Kong W, Li Q, Li X, et al. A biodegradable biomass-based polymeric composite for slow release and water retention. J Environ Manage. 2019. https://doi.org/10.1016/j.jenvman.2018.09.086.
7. Lado M, Ben-Hur M. Treated domestic sewage irrigation effects on soil hydraulic properties in arid and semiarid zones: a review. Soil Tillage Res. 2009. https://doi.org/10.1016/j.still.2009.04.011.
8. Li H, Li T, Jiang R, et al. A new method to simultaneously measure the soil-water characteristic curve and hydraulic conductivity function using filter paper. Geotech Test J. 2020. https://doi.org/10.1520/GTJ20190162.
9. Li L, Yuan Z, Li F. Changes in soil aggregates composition stabilization and organic carbon during deterioration of alpine grassland. IOP Conf Ser Earth Environ Sci. 2019. https://doi.org/10.1088/1755-1315/237/3/032068.

10. Ma Li, Wang Q, Shen S. Response of soil aggregate stability and distribution of organic carbon to alpine grassland degradation in Northwest Sichuan. Geoderma Reg. 2020. https://doi.org/10.1016/j.geodrs.2020.e00309.
11. Ning L, Shi H, Zhou H, Liu S. Quantitative characteristics of soil aggregates under different vegetations in upper reach of Minjiang river. Chin J Appl Ecol. 2005;16(8):1405–10.
12. Qin F, Ge H, Yan F, Chang G. Analysis and application of ecological protection technique for slope protection in mountainous area expressway. Appl Mech Mater. 2012. https://doi.org/10.4028/www.scientific.net/AMM.178-181.1545.
13. Schönbrodt S, Saumer P, Behrens T, et al. Assessing the USLE crop and management factor C for soil erosion modeling in a large mountainous watershed in central China. J Earth Sci. 2010. https://doi.org/10.1007/s12583-010-0135-8.
14. Shi H, Shao HB. Modifying transition matrix to evaluate soil quality: a case study in karst region in the west-southern china. Clean: Soil, Air, Water. 2012. https://doi.org/10.1002/clen.201100072.
15. Sojka RE, Bjorneberg DL, Entry JA, et al. Polyacrylamide in agriculture and environmental land management. Adv Agron. 2007. https://doi.org/10.1016/S0065-2113(04)92002-0.
16. van Genuchten MT. A closed-form equation for predicting the hydraulic conductivity of unsaturated soils. Soil Sci Soc Am J. 1980. https://doi.org/10.2136/sssaj1980.03615995004400050002x.
17. Wang Z, Yang JX, Kuang JJ, et al. Application of filter paper method in field measurement of matric suction. Chin J Geotech Eng. 2003;25(4):405–8 (**Yantu Gongcheng Xuebao**).
18. Wei S, Zhang X, McLaughlin NB, et al. Impact of soil water erosion processes on catchment export of soil aggregates and associated SOC. Geoderma. 2017. https://doi.org/10.1016/j.geoderma.2017.01.021.
19. Wu H, Liu J, Zhang Z, et al. Responses of effective soil water content to accumulative effect of vegetation growth in songshan nature reserve. Vegetos. 2013. https://doi.org/10.5958/j.2229-4473.26.1.040.
20. Yang CD, Lu SG. Effects of five different biochars on aggregation, water retention and mechanical properties of paddy soil: a field experiment of three-season crops. Soil Tillage Res. 2021. https://doi.org/10.1016/j.still.2020.104798.
21. Yang YH, Wu JC, Zhao SW. Effects of different macromolecule absorbent resins on the moisture characteristics of major soil type on loess plateau. Asian J Chem. 2014. https://doi.org/10.14233/ajchem.2014.18198.
22. Zhang M, Yang P, Lan G, et al. High crosslinked sodium carboxyl methylstarch-g-poly (acrylic acid-co-acrylamide) resin for heavy metal adsorption: its characteristics and mechanisms. Environ Sci Pollut Res. 2020. https://doi.org/10.1007/s11356-020-09945-0.
23. Zhao J, Deng P, Chen S. Structural characteristics of the fly ash wrapped by the super absorbent resin among the plant fiber and the application research on the complex. Mater Sci Forum. 2011. https://doi.org/10.4028/www.scientific.net/MSF.685.272.

Publisher's Note